Functionally Graded Material Production and Characterization using the Vertical Separator Molding Technique and the Powder Metallurgy Method

I. Kayabasi
Motor Vehicles and Transportation Technology Department
Küre Vocational School of Higher Education
Kastamonu University
Kastamonu, Turkey
ikayabasi@kastamonu.edu.tr

G. Sur
Mechanical Engineering Department
Engineering Faculty
Karabuk University
Karabuk, Turkey
gokhansur@karabuk.edu.tr

H. Gokkaya
Mechanical Engineering Department
Engineering Faculty
Karabuk University
Karabuk, Turkey
hgokkaya@karabuk.edu.tr

Y. Sun
Metallurgy and Materials Engineering Department
Engineering Faculty
Karabuk University
Karabuk, Turkey
ysun@karabuk.edu.tr

Received: 28 April 2022 | Revised: 12 May 2022 | Accepted: 15 May 2022

Abstract-Functionally Graded Materials (FGMs) are advanced customized engineering materials that gradually and continuously change their composition. The current study investigated the production feasibility and some post-production mechanical/physical properties of B_4C particle-reinforced (avg. 40μm) AA7075 matrix (avg. 60μm) FGM composites with the vertical separator molding technique using the high-temperature isostatic pressing powder metallurgy method. FGMs produced consist of three (0 – 30 – 60 wt. % B_4C) and four (0 – 20 – 40 – 60 wt. % B_4C) layers. The powders were mixed in a power blender mixer for 2h and were placed in the mold sections with a vertical separator. The lid was closed, and a pre-pressure of 10Mpa was applied. The FGM green sheet was transferred from the vertical separator mold to the hot work tool steel with a press. In this mold, FGMs were sintered at 560°C for 30 min under a pressure of 325MPa. Microstructural examinations did not reveal any separation or crack formation in the layer transition regions of the FGMs. In addition, a relatively homogeneous B_4C reinforcing distribution was observed in the layers with a low reinforcement ratio (wt. 20% and 30%) compared to the other layers. The highest hardness was 170 HBN in one layer of the four-layer FGM containing 40% by weight B_4C reinforcement. The highest transverse rupture strength was measured in the test performed from the region with the most reinforcement of the four-layer FGM at 482MPa.

Keywords-functionally graded material; powder metallurgy; hot pressing; transverse rupture strength

I. INTRODUCTION

FGMs are widely used in various fields such as aerospace, automotive, electronics, defense industry, gas turbine engines, and engineering applications. They have emerged as a relatively new material class [1, 2]. The FGMs are materials that change their composition and structure and seriously alter their material properties gradually along with their height [3, 4]. Functionally Graded Metal Matrix Composites (FGMMCs) with metal and ceramic content have great potential and importance for the fabrication and design of components and structures. FGMMCs have superior features to bring advanced engineering components to a better level along with material design. Specific properties such as high-temperature surface wear resistance, thermal mismatch correction, reduction of interfacial stresses, minimization of thermal stresses, increased metal-ceramic interfacial adhesion, delayed crack formation, and increased fracture toughness can be obtained by utilizing FGMMCs [1].

Aluminum Matrix Composite (AMC) is considered one of the most promising materials due to its lightweight and high specific strength values [5-7]. Among the existing AMCs, AA7075 is a matrix material with high strength, sufficient toughness, and corrosion resistance [8]. The vast-majority of reinforcing materials of AMCs are non-metallic ceramic materials. Al_2O_3, SiC, and B_4C are the most commonly used ceramic reinforcements in AMCs [9]. B_4C reinforcement material stands out among ceramics due to its good chemical inertness, high hardness, high elastic modulus, and high melting properties [10].

One of the most important areas in FGM research is the production method [1]. Many different fabrication methods have been developed to fabricate FGMs, such as gas-based

Corresponding author: I.Kayabasi

methods, liquid-phase methods, solid-phase methods, and biopolymeric-based functionally graded structures. Powder metallurgy, one of the solid phase methods, is a good method for obtaining a homogeneous and graded structure in FGM production [11, 12]. The powder metallurgy method offers advantages such as low processing temperature, ease of obtaining the final product, continuity in product quality, and low cost with its suitability for mass production compared to melting methods [13, 14]. In FGM production by powder metallurgy method, powders are gradually laid into the mold according to the reinforcement ratio [15]. This process is mostly carried out based on one's dexterity. It is difficult to obtain a smooth transition surface between layers in such manual procedures. In FGM production with another powder metallurgy method, the powder is laid in the mold for each stage and subjected to pre-pressing [16, 17]. This adversely affects the formation of the desired bond structure on the layer transition surfaces during the sintering phase. Vertical separator molding technique has been developed in order to obtain a smoother transition zone, to create the desired bond structure in the layer transition zones, and to provide the layer transition zones in the desired two-dimensional geometric structures.

In this study, a two-stage mold consisting of a vertical separator, a filling chamber, and a hot-pressing mold was designed and manufactured for FGM production under the high temperature isostatic pressing technique of the powder metallurgy method. The availability of planeness of transition surfaces of the B_4C reinforced AA7075 matrix FGMs with 3 (0-30-60% wt.) and 4 (0-20-40-60% wt.) layers of the same thickness as the manufactured mold was examined, along with the post-production metallurgical and mechanical properties.

II. MATERIALS AND METHODS

This study was carried out for FGM production. The chemical composition of AA7075 matrix (avg. 60μm) is presented in Table I. Reinforcement material B_4C (avg. 40μm) powder was used.

TABLE I. CHEMICAL COMPOSITION OF AA7075

Element	Zn	Mg	Cr	Cu	Fe	Si	Mn	Ti	Al
%Avg.	5.5	2.5	2.5	1.6	0.5	0.4	0.3	0.2	Bal.

The Scanning Electron Microscopy (SEM) images of matrix and reinforcement are shown in Figure 1. SEM investigations showed that AA7075 powder was relatively spherical in shape and variable in grain size. It has been observed that the reinforcement B_4C powder was composed of particles with complex geometry and sharp edges, whose aspect ratio is relatively close to each other.

In determining the percent weight ratio of the reinforcement of the FGM layers, one side is designed in a brittle structure with a high reinforcement ratio (high hardness, high wear resistance, high compressive strength), and the other side is designed in a tensile structure without reinforcement (high toughness, high % elongation). Information about the number of layers and reinforcement content of the produced FGMs are presented in Table II.

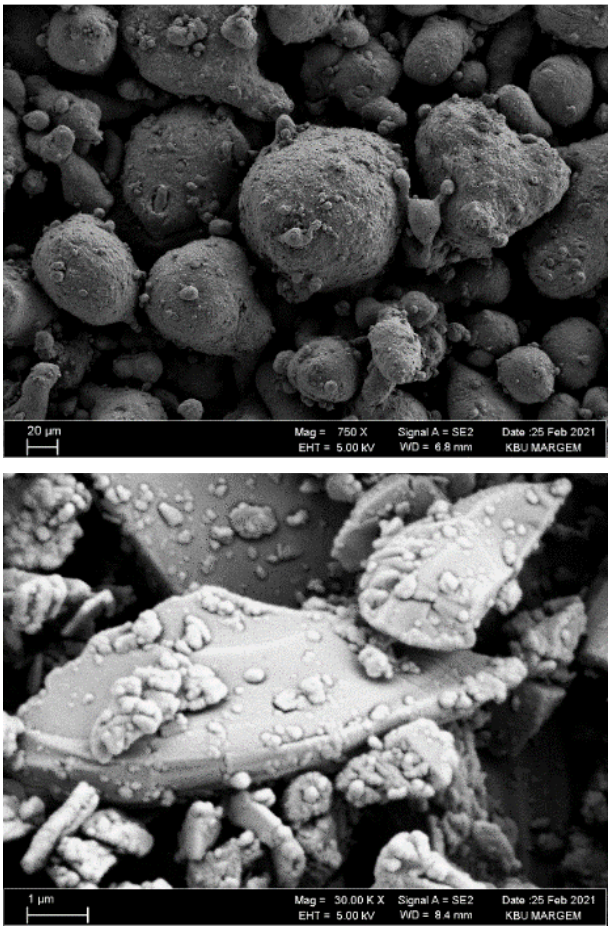

Fig. 1. SEM images of the powders used in FGM production: (a) AA7075, (b) B_4C.

TABLE II. LAYER AND REINFORCEMENT RATIOS OF THE PRODUCED FGMS

Number of layers	**3**	**4**
Layer reinforcement rates (% wt.)	0 – 30 – 60	0 – 20 – 40 – 60

Under the ratios in Table II, matrix and reinforcement powders were weighed on a precision balance at suitable values for the mixing ratio of each layer. In order to obtain a homogeneous powder mixture, it was mixed in a power mix blender for 2 hours. The mixed powders were filled into mold chambers (3 layers 60×60×8mm, 4 layers 60×60×6mm), whose layer areas were separated in equal volume by vertical steel separators. After the powder filling process, the steel separators were removed, the upper surface of the mold was closed, and a pre-compression force of 10MPa was applied under uniaxial hydraulic press. The pre-compression force was applied from the surface of the layer with the highest reinforcement ratio (60% wt. B_4C). Pre-compressed green sheet FGM was transferred into a separate mold made of hot work tool steel using a hydraulic press to carry out high-temperature isostatic pressing and sintering processes. Green sheet FGM samples were heated up to 560°C in a hot work tool steel mold and waited for 30min. Then, sintering was carried out at this temperature for 30min under a pressure of 325MPa and the samples were left to cool in the mold at room temperature. At

least two FGM samples were produced from each layer number. The samples were 60×60×12.7 ±0.13mm in size. The produced FGM samples and the cross-sectional macro views of the 3 and 4 layered samples are shown in Figure 2. The microstructure characterization of the produced FGM samples was investigated using the FEI QUANTA FEG 250 SEM located in Kastamonu University Central Research Laboratories and Research Center. The hardness values of the layers of the FGMs were determined by the Brinell hardness measurement method using the QNESS Q250M type hardness measuring device at Karabuk University's Iron and Steel Institute.

Fig. 2. FGM sample images: (a) After sintering, (b) 3-layer cross-sectional view, (c) 4-layer cross-sectional view.

FGM hardness measurements were carried out using 2.5mm diameter steel balls under a 62.5kg load. At least 5 measurements were made for each layer of the FGM, and the average determined the hardness value for the general layer. The produced FGMs were cut according to the ASTM B528-05 standard (31.9×12.7×12.7±0.13mm) and turned into transverse rupture strength test specimens. Transverse rupture strength tests were performed on the cut samples in a 50kN capacity INSTRON 3369 tension/compression device. Transverse rupture strength tests were performed at a deformation rate of 2mm/min. Transverse rupture strength load was applied separately to the layer surface of the FGM with the highest reinforcement and to the layer surface without reinforcement. The transverse rupture strength test results were determined by the average of the measurements after at least 4 measurements in each direction.

III. RESULTS AND DISCUSSION

A. *Microstructure Results*

SEM images of each layer and the interlayer transition zones were taken to determine the microstructure properties of the produced FGMs. SEM images are given in Figure 3 for the 3-layer FGM and Figure 4 for the 4-layer FGM.

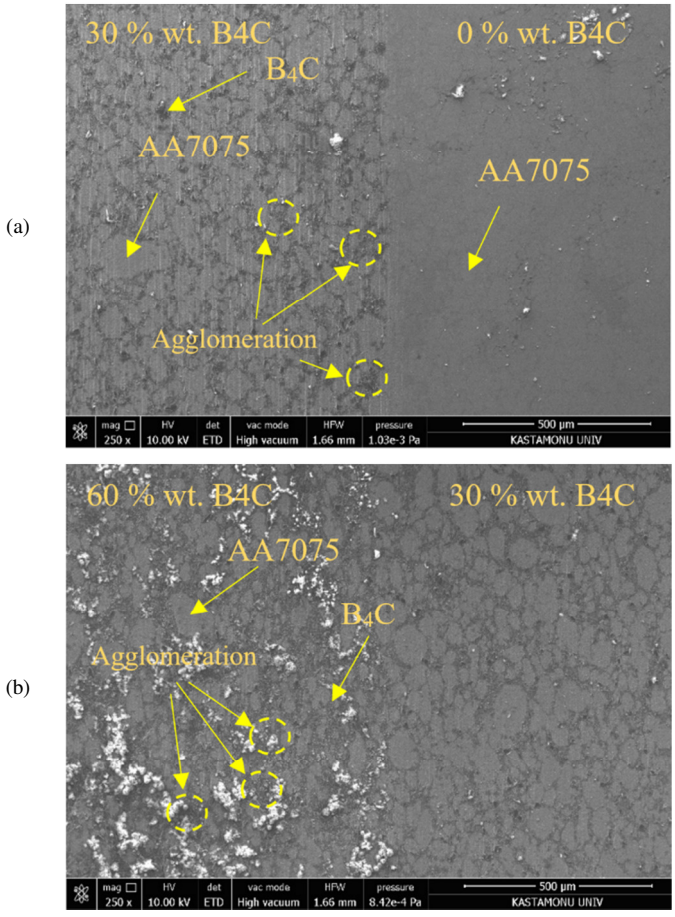

Fig. 3. SEM microstructure images of 3-layer FGMs: (a) 0% to 30% wt. B_4C transition surface image, (b) 30% to 60% wt. B_4C transition surface image.

It was determined that B_4C reinforcement in FGMs settled at grain boundaries and showed a relatively homogeneous distribution in low-rate layers. It was observed that B_4C reinforcement accumulated at the grain boundary with increasing reinforcement ratios. It is not easy to obtain a homogeneous distribution while producing composite materials with the powder metallurgy technique because the reinforcement can settle at the grain boundaries.

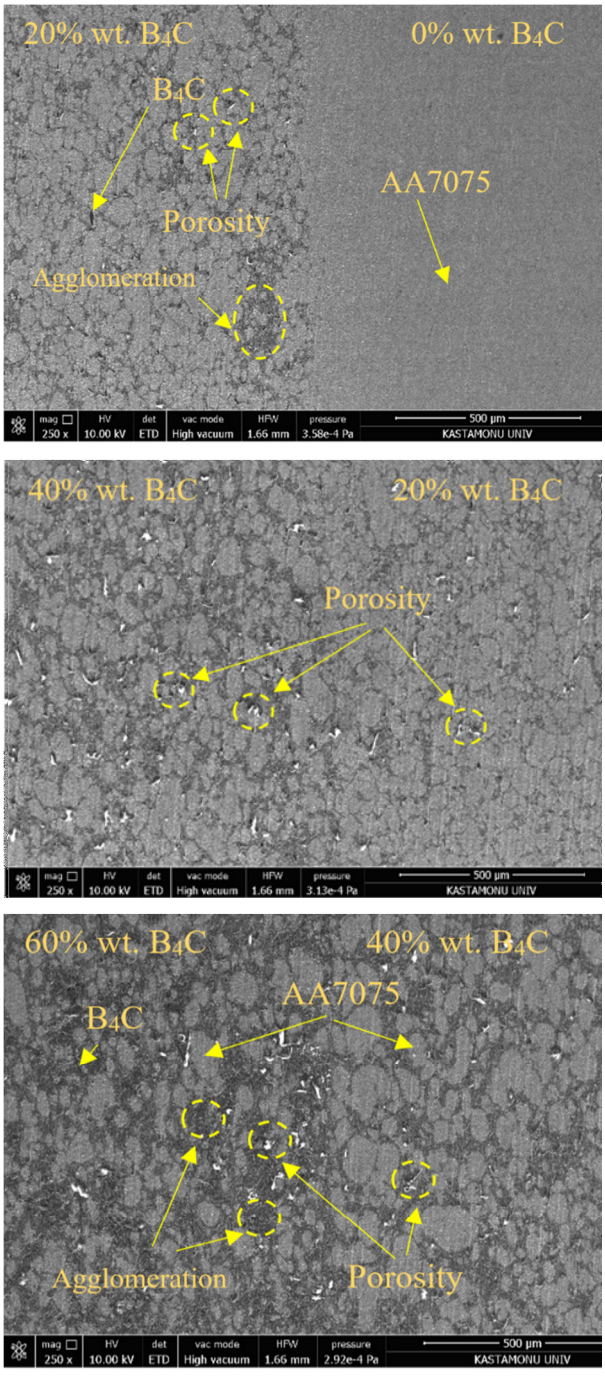

Fig. 4. SEM microstructure images of 4-layer FGMs: (a) 0% to 20% wt. B_4C transition surface image, (b) 20% to 40% wt. B_4C transition surface image, (c) 40% to 60% wt. B_4C transition surface image.

In addition, it has been reported that the porosity increases due to the increasing reinforcement ratio [1, 18]. It was determined that agglomeration and micropores increased as the amount of reinforcement increased in the layers of the produced FGMs. When the transition zones between the layers of the produced FGMs were examined, no delamination was observed. It has been observed that the transition of FGM between layers is continuous and has structural integrity.

B. Hardness Results

It has been reported that the hardness value increases with the increase of the ratio in the reinforcement structure in composite materials up to certain values [19-22]. The hardness measurements performed on the layers of the produced FGM samples showed that the hardness value increased up to 40% wt. B_4C, and after this value, it decreased depending on the decreasing matrix amount and increasing porosity. Similarly, in [15], the measured hardness value was 40% wt. Graphs of change in the hardness (Brinell; HBN) values of each layer depending on the number of layers of FGMs are presented in Figure 5.

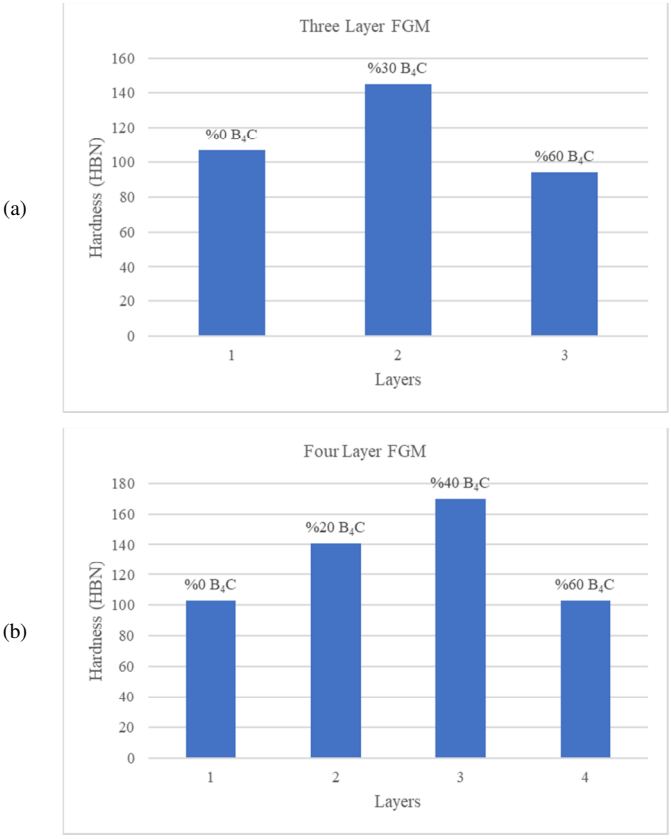

Fig. 5. Layer hardness of FGMs: (a) 3-layer, (b) 4-layer.

It can be seen in Figure 5 that the hardness increases to a certain extent (30% wt. B_4C in 3 layers and 40% wt. B_4C in 4 layers) depending on the increase of layer reinforcement. Suppose a composite is produced with success within the desired limits (homogeneous distribution property, porosity amount, etc.) of composite materials. In that case, it is expected

that the mechanical properties and hardness values will increase according to the mixture theory as the reinforcement ratio increases up to a certain value. Equation (1) presents the mathematical expression used to theoretically calculate the hardness of the composites according to the mixture theory.

$$H_K = H_m f_m + H_t f_t \quad (1)$$

where H_k is the hardness of the composite, H_m is the hardness of the matrix, f_m is the weight ratio of the matrix, H_t is the reinforcement hardness, and f_t is the reinforcement by weight ratio.

It was determined that the layer with the highest hardness value of the produced FGMs was the third layer of the 4-layer FGM reinforced with 40%wt. B_4C. The hardness of this layer was measured as 170HBN. The lowest hardness value was 94HBN in the layer with the highest reinforcement ratio (60% wt.) of the 3-layer composite. When the SEM images of the 3- and 4-layer FGMs in Figure 3 and Figure 4 are examined, it was seen that the 60% wt. B_4C reinforced layer had the highest porosity. Therefore, Brinell's hardness decreased in layers containing 60% wt. B_4C reinforcement.

C. Transverse Rupture Strength Tests Result

In order to determine the breaking strength of FGMs, transverse rupture strength test was performed on reinforced and non-reinforced layer surfaces under test conditions prepared under the ASTM B528-05 standard. The flexure stress-strain graphs obtained as a result of the experiments are presented in Figure 6. It can be seen in Figure 6 that the transverse rupture strength of FGMs differs according to the region where the load is applied. The measured transverse rupture strength of the FGM was higher (~153% in the 3-layer, ~65% in the 4-layer composite) with the application of the fracture load from the dense region of the reinforcement, because composites are more resistant to compressive stresses [23]. The highest obtained transverse rupture strength was 482MPa, from a 4-layer FGM applied to the load region with the highest number of reinforcement. In Figure 6(b), 4-layer FGM transverse ruptured from the region with less reinforcement showed brittle fracture than the 3-layer FGM due to the decreased amount of matrix due to the layer increase. The increase in strength in composites can be explained according to the law of mixtures. Equation (2) shows the strength increase in composite materials according to the law of mixtures [24, 25].

$$\sigma_K = \sigma_m f_m + \sigma_t f_t \quad (2)$$

where σ_K refers to the mechanical strength of the composite, σ_m refers to the mechanical strength of the matrix, f_m refers to the weight ratio of the matrix, σ_t refers to the mechanical strength of the reinforcement, and f_t refers to the weight ratio of the reinforcement. This equation predicts the strength values when the composite is produced within the desired limits without exceeding the ideal production conditions. As the ratio of the side with a higher strength value compared to others increases, the strength of the composite also increases.

It was observed that the porosity increased as the amount of reinforcement increased, in accordance with [1, 15]. The highest Brinell hardness in FGM was obtained in the 40% wt. B_4C layer. As the reinforcement ratio increased, the hardness of the composite decreased. Similar results were found in [1]. The best results in the transverse rupture strength test were obtained on the reinforced layer surface. Similar results were obtained in [15].

(a)

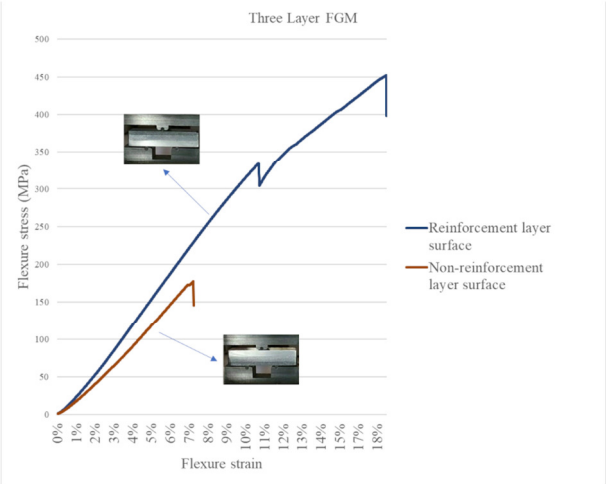

(b)

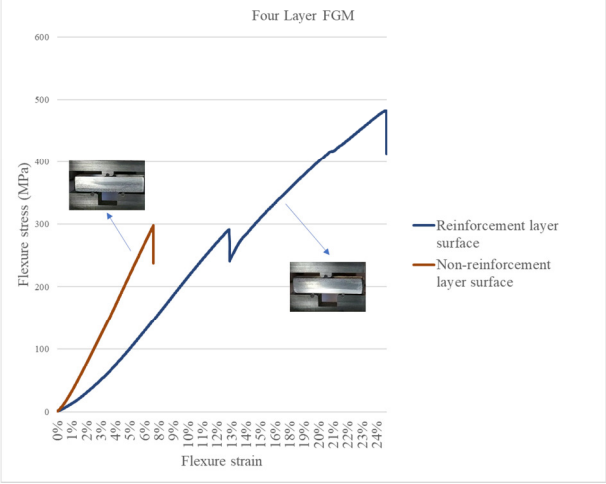

Fig. 6. FGM transverse rupture strength graphics: (a) 3-layer, (b) 4-layer.

IV. CONCLUSIONS

This study produced 3 (0-30-60% wt.) and 4 (0-20-40-60 wt.%) layers of B_4C reinforced AA7075 matrix FGM with the vertical separator moulding technique. The following results were obtained in this study, in which the microstructure characterization, hardness and transverse rupture strength of the produced FGMs were examined.

- With the vertical separator moulding technique, FGMs with smooth surface transition were successfully produced without any delamination in the transition areas.
- It was determined that the distribution of B_4C reinforcement in the layers of FGMs with a low reinforcement ratio (wt. 20% and 30%) was relatively homogeneous compared to the other layers.
- No delamination was observed between the layers of FGM.

- The highest porosity was observed in the layer containing 60 wt.% B_4C. The lowest measured Brinell hardness was 92HBN in the 3-layer FGM containing 60% wt. B_4C reinforcement.
- The highest measured Brinell hardness was 170HBN in the 4-layer FGM containing 40% wt. B_4C reinforcement.
- In terms of transverse rupture strength, the tests applied to the reinforcement layer surface gave better results than the tests applied to the non-reinforcement layer surface (~153% in three layers, ~65% in four layers).
- The greatest measured transverse rupture strength was 482MPa due to the application of the load from the region of the 4-layer FGM with the highest reinforcement.

REFERENCES

[1] F. Erdemir, A. Canakci, and T. Varol, "Microstructural characterization and mechanical properties of functionally graded Al2024/SiC composites prepared by powder metallurgy techniques," *Transactions of Nonferrous Metals Society of China*, vol. 25, no. 11, pp. 3569–3577, Nov. 2015, https://doi.org/10.1016/S1003-6326(15)63996-6.

[2] G. Udupa, S. S. Rao, and K. V. Gangadharan, "Functionally Graded Composite Materials: An Overview," *Procedia Materials Science*, vol. 5, pp. 1291–1299, Jan. 2014, https://doi.org/10.1016/j.mspro.2014.07.442.

[3] R. Watanabe, T. Nishida, and T. Hirai, "Present status of research on design and processing of functionally graded materials," *Metals and Materials International*, vol. 9, no. 6, pp. 513–519, Dec. 2003, https://doi.org/10.1007/BF03027249.

[4] S. Agca and N. Akar, "Santrifuj Dokum Yontemiyle Uretilen Al-Cu Fonksiyonel Derecelenmis Malzemelerde Uretim Parametrelerinin Malzemenin Sertligi Uzerine Etkisi," *Politeknik Dergisi*, vol. 20, no. 1, pp. 121–127, 2017, https://doi.org/10.2339/2017.20.1.

[5] A. S. Alghamdi, M. Ramadan, K. S. A. Halim, and N. Fathy, "Microscopical Characterization of Cast Hypereutectic Al-Si Alloys Reinforced with Graphene Nanosheets," *Engineering, Technology & Applied Science Research*, vol. 8, no. 1, pp. 2514–2519, Feb. 2018, https://doi.org/10.48084/etasr.1795.

[6] A. Ugur, H. Gokkaya, G. Sur, and N. Eltugral, "Friction Coefficient and Compression Behavior of Particle Reinforced Aluminium Matrix Composites," *Engineering, Technology & Applied Science Research*, vol. 9, no. 1, pp. 3782–3785, Feb. 2019, https://doi.org/10.48084/etasr.2507.

[7] R. R. Liu, C. Wu, J. Zhang, G. Luo, Q. Shen, and L. Zhang, "Microstructure and mechanical behaviors of the ultrafine grained AA7075/B4C composites synthesized via one-step consolidation," *Journal of Alloys and Compounds*, vol. 748, pp. 737–744, Jun. 2018, https://doi.org/10.1016/j.jallcom.2018.03.152.

[8] A. Canakci and T. Varol, "Microstructure and properties of AA7075/Al–SiC composites fabricated using powder metallurgy and hot pressing," *Powder Technology*, vol. 268, pp. 72–79, Dec. 2014, https://doi.org/10.1016/j.powtec.2014.08.016.

[9] M. Patel, S. K. Sahu, M. K. Singh, and N. Dalai, "Micro-structural and mechanical characterization of stir cast AA5052/B4C metal matrix composite," *Materials Today: Proceedings*, vol. 56, pp. 1129–1136, Jan. 2022, https://doi.org/10.1016/j.matpr.2021.10.331.

[10] H. Jin, S. Li, and Q. Ouyang, "Fabrication of Double-Layer 2024Al-2024Al/B_4C Composite by Plasma Activated Sintering and Its Mechanical Properties," *Engineering Science*, vol. 2, no. 1, Jan. 2017, Art. no. 1, https://doi.org/10.11648/j.es.20170201.11.

[11] M. S. Surya and G.Prasanthi, "Manufacturing and Micro structure study of Al-SiC Functionally graded material," *Materials Today: Proceedings*, vol. 4, no. 2, Part A, pp. 621–627, Jan. 2017, https://doi.org/10.1016/j.matpr.2017.01.065.

[12] A. Pasha, B. M. Rajaprakash, "Functionally graded materials (FGM) fabrication and its potential challenges & applications," *Materials Today: Proceedings*, vol. 52, pp. 413–418, Jan. 2022, https://doi.org/10.1016/j.matpr.2021.09.077.

[13] K. H. Min, S. P. Kang, D.-G. Kim, and Y. D. Kim, "Sintering characteristic of Al2O3-reinforced 2xxx series Al composite powders," *Journal of Alloys and Compounds*, vol. 400, no. 1, pp. 150–153, Sep. 2005, https://doi.org/10.1016/j.jallcom.2005.03.070.

[14] V. C. Nguyen, T. D. Nguyen, and D. H. Tien, "Cutting Parameter Optimization in Finishing Milling of Ti-6Al-4V Titanium Alloy under MQL Condition using TOPSIS and ANOVA Analysis," *Engineering, Technology & Applied Science Research*, vol. 11, no. 1, pp. 6775–6780, Feb. 2021, https://doi.org/10.48084/etasr.4015.

[15] T. Yıldız and G. Sur, "Investigation of drilling properties of AA7075/Al2O3 functionally graded materials using gray relational analysis," *Proceedings of the Institution of Mechanical Engineers, Part B: Journal of Engineering Manufacture*, vol. 235, no. 9, pp. 1384–1398, Jul. 2021, https://doi.org/10.1177/0954405421995657.

[16] P. Kumar Chauhan and S. Khan, "Microstructural examination of aluminium-copper functionally graded material developed by powder metallurgy route," *Materials Today: Proceedings*, vol. 25, pp. 833–837, Jan. 2020, https://doi.org/10.1016/j.matpr.2019.10.007.

[17] R. Gunes, M. Aydin, M. Kemal Apalak, and J. N. Reddy, "Experimental and numerical investigations of low velocity impact on functionally graded circular plates," *Composites Part B: Engineering*, vol. 59, pp. 21–32, Mar. 2014, https://doi.org/10.1016/j.compositesb.2013.11.022.

[18] K. Rajasekhar, V. Suresh Babu, and M. J. Davidson, "Microstructural and mechanical properties of Al-Cu functionally graded materials fabricated by powder metallurgy method," *Materials Today: Proceedings*, vol. 41, pp. 1156–1159, Jan. 2021, https://doi.org/10.1016/j.matpr.2020.09.157.

[19] Md. H. Rahman and H. M. M. A. Rashed, "Characterization of Silicon Carbide Reinforced Aluminum Matrix Composites," *Procedia Engineering*, vol. 90, pp. 103–109, Jan. 2014, https://doi.org/10.1016/j.proeng.2014.11.821.

[20] M. P. Reddy *et al.*, "Enhanced performance of nano-sized SiC reinforced Al metal matrix nanocomposites synthesized through microwave sintering and hot extrusion techniques," *Progress in Natural Science: Materials International*, vol. 27, no. 5, pp. 606–614, Oct. 2017, https://doi.org/10.1016/j.pnsc.2017.08.015.

[21] B. N. Anil Kumar, A. Ahamad, and H. N. Reddappa, "Impact of B4C reinforcement on tensile and hardness properties of Al-B4C metal matrix composites," *Materials Today: Proceedings*, vol. 52, pp. 2136–2142, Jan. 2022, https://doi.org/10.1016/j.matpr.2021.12.454.

[22] U. K. Annigeri and G. B. Veeresh Kumar, "Effect of Reinforcement on Density, Hardness and Wear Behavior of Aluminum Metal Matrix Composites: A Review," *Materials Today: Proceedings*, vol. 5, no. 5, Part 2, pp. 11233–11237, Jan. 2018, https://doi.org/10.1016/j.matpr.2018.02.002.

[23] P. Shantharaj, A. S. Prashanth, M. Nagaral, V. Bharath, V. Auradi, and K. Dharshan, "Microstructure, tensile and compression behaviour of B4C particles reinforced Al7075 matrix composites," *Materials Today: Proceedings*, vol. 52, pp. 1135–1139, Jan. 2022, https://doi.org/10.1016/j.matpr.2021.11.008.

[24] W. S. AbuShanab, E. B. Moustafa, E. Ghandourah, and M. A. Taha, "Effect of graphene nanoparticles on the physical and mechanical properties of the Al2024-graphene nanocomposites fabricated by powder metallurgy," *Results in Physics*, vol. 19, Dec. 2020, Art. no. 103343, https://doi.org/10.1016/j.rinp.2020.103343.

[25] W. D. Callister Jr and D. G. Rethwisch, *Materials Science and Engineering: An Introduction*, 9th edition. Hoboken, NJ, USA: Wiley, 2013.